

## Photorefractive fixed optical correlator

E.M. de Miguel-Sanz<sup>1</sup>, M. Tebaldi<sup>2</sup>, S. Granieri<sup>2</sup>, N. Bolognini<sup>2</sup>, L. Arizmendi<sup>1</sup>

<sup>1</sup>Dept. Física de Materiales, Universidad Autónoma de Madrid, Cantoblanco, E-28049 Madrid, Spain  
(Fax: +34-91/397-8579, E-mail: luis.arizmendi@uam.es)

<sup>2</sup>Centro de Investigaciones Ópticas, CIOp (CONICET, CIC) and OPTIMO (Dpto. de Fisicomatemática, Facultad de Ingeniería, UNLP)  
Casilla de Correo 124, 1900 La Plata, Argentina (E-mail: postmaster@ciop.edu.ar)

Received: 10 May 1999/Revised version: 21 June 1999/Published online: 16 September 1999

**Abstract.** A photorefractive optical correlator stored and fixed in lithium niobate is presented. The device shows good correlation characteristics together with very high output efficiency and insensitivity to optical erasure during read-out.

**PACS:** 42.40.Pa; 42.70.Ln; 42.70.Nq; 42.79.Hp

The use of photorefractive crystals to synthesize large-capability spatial filters has played a crucial role in the development of real-time correlators [1, 2]. The main features of employing thick photorefractive materials for the matched-filter implementation are the large information capacity and high diffraction efficiency.

Although thick photorefractive crystals are promising in application to large-storage-capability holographic memories, the performance of the photorefractive matched filter is constrained by the Bragg condition. This determines the angular selectivity of the filter and affects its shift tolerance. This also provides the possibility for multiple pattern-matched-filter construction.

In degenerated wave-mixing experiments with a photorefractive crystal, the hologram is partially erased because the read-out wavelength is the same as that of the write-in beams, and then the diffraction efficiency is reduced. That is the read-out is destructive and the stored gratings are all progressively erased during this process. This problem can be partially solved by using for read-out a wavelength to which the crystal is not very sensitive. Nevertheless, over many cycles and particularly when using strong beams this procedure is still destructive. Moreover, this cannot be considered as a solution when one of the beams carries spatial information, i.e. when an image is stored, because a reading beam with different wavelength matched to the Bragg condition for the main grating  $k$ -vector will not match with other image  $k$ -vectors.

The gradual erasure of holograms stored in photorefractive materials during the read-out process is due to the effect of charge redistribution produced by the reading light. A procedure to improve the practical lifetime of these holograms is to undergo a fixing treatment. In lithium niobate a thermal

fixing process was found by Amodei and Staebler [3]. This process consists in heating the sample, after or during hologram recording, to a temperature in the range 120–180 °C for several minutes. When the sample is next cooled down and illuminated with uniform light, the hologram can be read without loss of diffracted intensity. The explanation of this effect is the following: (i) Compensation of the electric charge distribution of the hologram by ions which are mobile at high temperature. (ii) Freezing at room temperature of the ions in the new positions. At this stage the electronic grating ( $\text{Fe}^{2+}$ - $\text{Fe}^{3+}$  distribution) and the ionic grating are almost completely compensated. Diffracted light is not observed at this moment. (iii) Illumination with uniform light produces a partial erasure of the electronic grating, leaving part of the ionic charge uncompensated. This step is known as developing process. The ionic charge distribution forms a replica of the initial holographic grating having identical diffraction properties. It seems proved that  $\text{H}^+$  are the ions that are mobile at these relatively low temperatures and are responsible for thermal fixing [4]. A certain quantity of hydrogen is already present in all lithium niobate samples from the crystal growth process.

High developed refractive index change can be obtained when the recording is made at fixing temperature, leading to a diffraction efficiency close to 100% in samples of 1–2 mm thick [5]. Taking advantage of this characteristic, permanent diffraction-based devices can be produced by using fixed holograms in lithium niobate. Among them are multiplexers, pattern recognition devices, narrow bandwidth filters [6], time modulators [7], or optical correlators as proposed in this paper.

Of course, one must expect some long-time degradation of fixed holograms even at low temperatures. Ions have a very low but not negligible migration rate at RT. The lifetime of fixed holograms was determined to be also dependent on grating spacing [8]. For spacing of a few  $\mu\text{m}$  the lifetime at RT is a few years. By decreasing the writing angle a substantial increase in lifetime results. These data are relevant for the design of permanent diffractive devices.

The purpose of this paper is to present an optical correlator where the matched filter is written and fixed in  $\text{LiNbO}_3:\text{Fe}$ . This fixed correlator yields new possibilities for

many optical applications, in particular those requiring stability after the matched filter is fixed but not requiring to be modified for a long time. In Sect. 1 the operation of the Van der Lugt correlators is outlined and in Sect. 2 the experimental arrangement and the performance of the system are analyzed.

## 1 Optical correlator in a volume media: basic principles

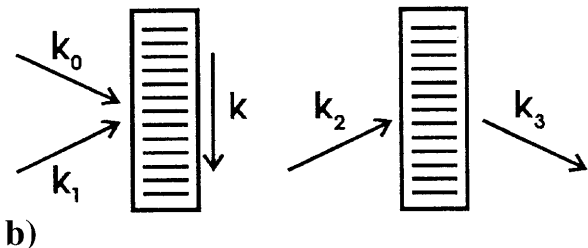
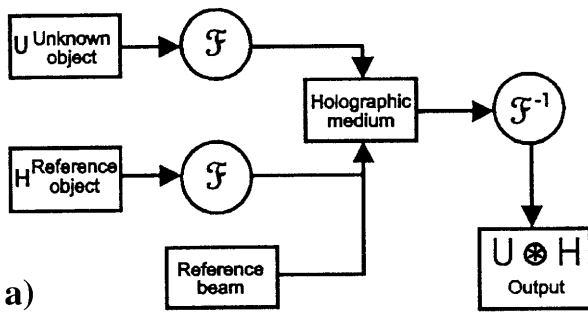
A correlator serves to compare an unknown object  $U_0$  with a known reference object  $H$ . Van der Lugt has shown how that can be optically done [9, 10]. Figure 1a shows the flow diagram of the Van der Lugt correlator based on the correlation theorem:

$$U_0 \otimes H = \mathcal{F}^{-1} \{ \mathcal{F}\{U_0\} \cdot \mathcal{F}\{H\} \}, \quad (1)$$

where  $U_0$  and  $H$  represent two-dimensional objects, and  $U_0 \otimes H$  represents the correlation function of  $U_0$  and  $H$ , which is given by

$$U_0 \otimes H = \int_{-\infty}^{\infty} \int_{-\infty}^{\infty} U_0(x', y') H(x' - x, y' - y) dx' dy'. \quad (2)$$

The advantage of (1) is that it contains the Fourier transform of  $U_0$  and  $H$  which is optically implemented by using lenses. Besides, the multiplication appearing on the right side of (1) can be done by means of a hologram using both the writing and reading processes. In this case, the result is proportional to the intensity of the diffracted beam in the reading process. In the Van der Lugt correlator the hologram is written by the interference of the Fourier transform of the reference object and a reference beam, usually a plane wave. The readout is done using as input beam the Fourier transform of the unknown object.



**Fig. 1.** **a** Flow diagram for the correlation operation. **b** Scheme of wave vectors corresponding to the matched filter storage and diffraction steps

The optical correlators based on the (1), like the Van der Lugt correlator, are neither rotation- nor size-invariant because they perform template matching only, but they should be shift-invariant. However, a thick holographic material, like a photorefractive crystal, imposes the Bragg diffraction condition which reduces the shift invariance capability. This is due to the fact that when the object is transversely shifted, its Fourier transform formed by the lens remains in the same position but the angles of beams forming each point have changed. The effect of Bragg mismatch on the angular selectivity can be explained with the vectorial diagram [11] shown in Fig. 1b. The recorded spatial grating vector  $\mathbf{k}$  is

$$\mathbf{k} = \mathbf{k}_0 - \mathbf{k}_1, \quad (3)$$

where  $\mathbf{k}_0$  and  $\mathbf{k}_1$  are the wave vectors used in the writing process. If the volume hologram is readout using a beam with wave vector  $\mathbf{k}_2$ , and the scattered light beam is represented by  $\mathbf{k}_3$ , then the *optical path difference* of the scattered field can be written

$$OPD = \mathbf{k} \cdot \mathbf{r} - (\mathbf{k}_3 - \mathbf{k}_2) \cdot \mathbf{r} = \Delta \mathbf{k} \cdot \mathbf{r}, \quad (4)$$

where

$$\Delta \mathbf{k} = \mathbf{k}_0 - \mathbf{k}_1 + \mathbf{k}_2 - \mathbf{k}_3 \quad (5)$$

is the dephasing wave vector. This vector represents the Bragg diffraction mismatch. When the reading beam is matched with the writing beam, the dephasing wave vector is null. The amplitude field distribution for the scattered light, as a function of the wave vector  $\mathbf{k}_3$  and under weak diffraction condition, can be written as

$$U(\mathbf{k}_3) = C \int_V \exp(i \Delta \mathbf{k} \cdot \mathbf{r}) d\mathbf{r}^3, \quad (6)$$

where the integration domain is the volume of the hologram.

As can be seen from (6), the performance of a matched filter based on a photorefractive crystal will be strongly limited by the Bragg condition. This effect increments the angular selectivity of the matched filter with the consequent decreasing in its shift tolerance. If we consider the case of a non-slanted transmission-type spatial filter, by using the Kogelnik's wave-coupling theory [12], the normalized diffraction efficiency is:

$$\eta = \frac{\sin^2(v^2 + \xi^2)^{1/2}}{1 + \xi^2/v^2}, \quad (7)$$

with

$$v = \frac{\pi \Delta n d}{\lambda \cos \theta}, \quad \xi = \frac{2\pi n d \sin \theta}{\lambda} \Delta \theta. \quad (8)$$

$n$  and  $\Delta n$  are the refractive index and its variation,  $d$  the thickness of the crystal, and  $\theta$  and  $\Delta \theta$  are the internal angle between reference and object beams and the off-Bragg angle respectively. Under weak-coupling condition ( $|v| \ll \pi$ ), the first-order zeroes in (7) are obtained for  $|\xi| \approx \pi$ .

## 2 Experimental implementation

### 2.1 Write-in process and fixing

In the experiments, the Van der Lugt configuration in a transmission geometry was used. Figure 2 schematically describes the experimental set-up employed. In the process of recording the holographic filter the light from an Ar<sup>+</sup> laser with wavelength  $\lambda_w = 514.5$  nm was used. This process employs a lens  $L_1$  that generates the complex Fourier transform field of the reference object H which interferes with the reference plane wave in the sample of LiNbO<sub>3</sub> crystal. The resulting intensity distribution produces via the photorefractive effect a refractive index grating in the crystal.

A sample of congruent lithium niobate crystal doped with 0.1% mol of iron was used. This sample was 11 mm × 9 mm × 1 mm in size and was oriented with the *c* axis parallel to its large faces. From the absorption coefficient of  $\sim 1.7$  cm<sup>-1</sup> measured at 477 nm and using the absorption cross section for Fe<sup>2+</sup> given in [13] a reduction state of  $[\text{Fe}^{2+}]/[\text{Fe}^{3+}] \approx 0.02$  is estimated. Besides, from the infrared absorption band of OH<sup>-</sup> stretching resulted a hydrogen concentration [14] of  $[\text{H}^+] \approx (2.7 \pm 0.2) \times 10^{19}$  cm<sup>-3</sup>. The sample was short-circuited by covering its four lateral faces with conductive silver paint in order to avoid spatial charge accumulation at *c* axis ends due to the photovoltaic effect when the crystal is homogeneously illuminated.

For recording and fixing processes the sample was mounted in a metallic holder in contact with a heater. The temperature could be varied and controlled from RT to 300 °C with a precision of  $\pm 0.1$  °C. The sample and the heater were placed inside a vacuum chamber provided with large optical windows.

As mentioned, the sample was illuminated with a reference plane wave and the Fourier transform of a reference object. The reference wave had at least the same intensity as

the diffraction-limited zero-order spot of the Fourier transform, and covered all the sample face avoiding photovoltaic charge accumulation. The matched filter was stored and fixed simultaneously at 160 °C for 30 min. Another possibility is to store the hologram first at RT and after that produce the fixing by heating the sample at 160 °C for 30 min. However in this case the diffraction efficiency is low in comparison with the first procedure. Developing was produced by illuminating with white light of two 150-W halogen lamps focused to cover both faces of the sample to reach a stable diffraction level. In these experiments the mean crossing angle was 22°, corresponding to a main fringe spacing of  $\Lambda = 1.35$  μm. The lifetimes of fixed holograms depend on the temperature and the grating spacing. For this spacing and a temperature of 20 °C a hologram lifetime of  $\tau \cong 10$  years is estimated from an extrapolation of the data given in [8].

### 2.2 Read-out process

In the read-out process the Fourier transform of the unknown object is incident on the crystal plane at the Bragg angle, in order to maximize the diffracted intensity, as shown in Fig. 2b. In this process the same wavelength was used as in the write-in step without degrading the filter-matching characteristics. As was stated, the diffracted beam intensity is proportional to the correlation function of the reference and unknown objects. Finally, a CCD sensor located at the Fourier plane of a lens  $L_3$  captures the correlation peak which is then displayed on a monitor and stored as a file on a computer disk.

Table 1 shows the recognition performance of the correlator for different characters. The first and second columns display the reference and unknown character, respectively. The third and fourth columns show the output correlation peaks and the profile intensity plots, respectively. The difference in correlation response when the unknown character coincides or not with the reference one is well apparent.

By using a similar character as the reference object, it can be seen from Table 2 that the fixed optical correlator ex-

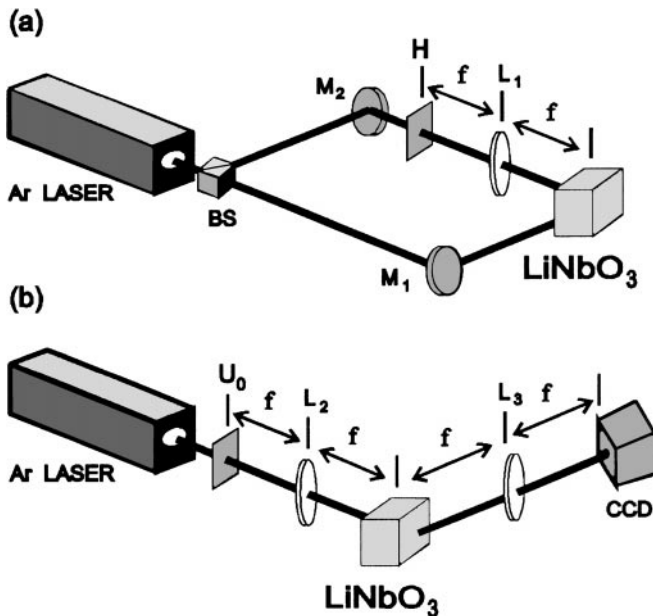

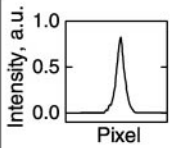

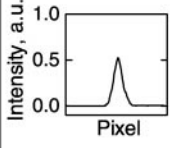

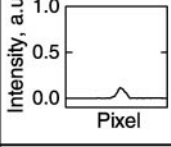

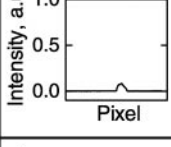

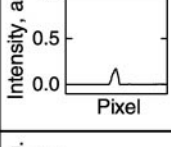

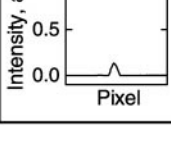


Fig. 2. **a** Write-in set-up for the matched filter. BS: beam splitter;  $M_1$ ,  $M_2$ : mirrors,  $L_1$ : lens (focal length: 50 cm), H: reference object. **b** Read-out set-up.  $U_0$ : unknown object;  $L_2$  and  $L_3$ , lenses (focal length: 50 cm)

Table 1. Photorefractive fixed correlator performance

Reference object	Unknown object	Correlation peak	
		output	profile
P	P		
P	E		
P	S		

**Table 2.** Non-rotation-invariance behaviour

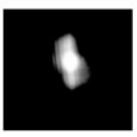
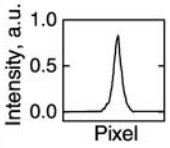

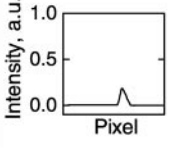
Reference object	Unknown object	Correlation peak	
		output	profile
P	P		
P	P (rotated)		
P	P (rotated)		
P	P (rotated)		
P	P (rotated)		
P	P (rotated)		

hibits lack of invariance when the object is rotated. In this way, it behaves as the conventional Van der Lugt correlator. Moreover it is shown in Table 3 that this configuration is not size-invariant. As can be observed in these tables, the correlator has a good signal-to-noise ratio which renders a remarkable discrimination of the detected signal.

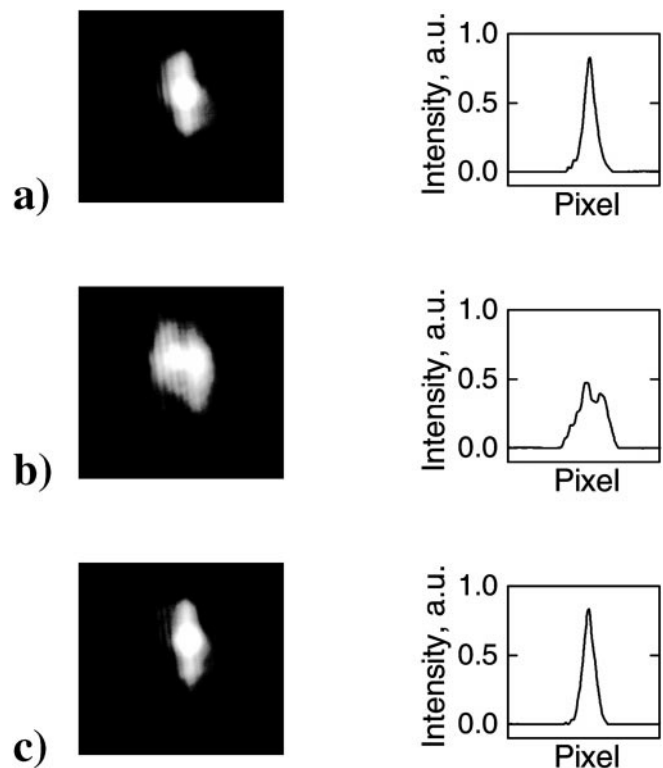
In order to determine the experimental shift tolerance of the correlator we have laterally moved the unknown object up to the position where the correlation beam disappeared. From maximum correlation position this displacement was  $\approx 0.8$  mm. Taking into account that the focal length of the Fourier transform lens was 50 cm, and considering that beams change small angles due to the displacement, we obtain an experimental angular selectivity of  $\Delta\theta \approx 7 \times 10^{-4}$  rad. In accordance with (7), the halfwidth of the Bragg diffraction peak resulted in  $\Delta\theta = 1.03 \times 10^{-3}$  rad for our experimental conditions. The 30% difference between these values could be due to the roughness of the experimental procedure.

The photorefractive effect is still present in LiNbO<sub>3</sub> samples having fixed holograms. During the hologram readout the Fourier transform of the unknown object is projected on the crystal to obtain the correlation output. This intensity dis-

**Table 3.** Non-size-invariance behaviour

Reference object	Unknown object	Correlation peak	
		output	profile
P	P		
P	P (smaller)		

tribution is formed by very focused beams located in small parts of the sample. The relatively high intensity concentrated at these spots also produces refractive index changes via the photorefractive effect. This leads after some reading time to distortions of the hologram fringes and hence to a degradation of the correlation results. Assuming that this distribution does not appreciably heat the illuminated portion of the sample, the index perturbation will be not fixed and can be erased with the proper uniform illumination after some reading time. The initial diffraction properties are then restored. If this non-coherent illumination is maintained during the reading time, then the distortion effect could be diminished or even avoided at all. In Fig. 3 these effects of degradation during the read-



**Fig. 3a–c.** Degradation effect due to the read-out beams and recovering of the initial performance after uniform illumination. **a** Initial correlation peak. **b** Degraded correlation. **c** Recovered output

out process and the retrieval after uniform illumination are shown. To this purpose, the autocorrelation of the character P is produced. In Fig. 3a the initial correlation output is presented. In Fig. 3b the correlation peak after a continuous reading of 30 min is shown. Finally, in Fig. 3c the reversible restoration of the initial correlation peak after 30 min of uniform white light illumination is observed. Note that these cycles of degradation–restoration are reversible processes which of course cannot be implemented in a non-fixed correlator.

### 3 Conclusions

To our knowledge, a photorefractive fixed optical correlator is presented for the first time. The fixing process allows the correlator to operate irrespective of the wavelength employed without decreasing the diffraction efficiency by optical erasure.

In a non-fixed photorefractive Van der Lugt correlator usually a non-sensitive read-out wavelength is employed to avoid hologram degradation. As a consequence, in this non-degenerate four-wave-mixing approach, since different wavelengths are used for the write-in and read-out process, then an accurate alignment of the read-out Fourier transform with the recorded filter is required. This problem is overcome by the fixing procedure because non-degradation appears even using the same wavelength in both the write-in and read-out steps.

The LiNbO<sub>3</sub> crystal showed a good performance in terms of diffraction efficiency. It was established that the fixing procedure after the write-in step is less efficient than the case in which both procedures are simultaneously done.

This correlator has the advantage that after the information is registered, the crystal is easily transportable and could be used in an industrial environment without the characteristic stability requirements of the usual non-fixed correlators.

*Acknowledgements.* The authors would like to acknowledge the partial support of this work by the Spanish Ministerio de Educación y Cultura under Programa de Cooperación Iberoamericana and grant no. PB97-0008. One of the authors (E.M.M.S.) is grateful to Caja Segovia for a research fellowship.

### References

1. D.T.H. Liu, L.J. Cheng: *Appl. Opt.* **31**, 5675 (1992)
2. H. Rajbenbach, S. Bann, P. Réfrégier, P. Joffre, J. Huignard, H. Buchkremer, A. Jensen, E. Rasmussen, K. Brenner, G. Lohman: *Appl. Opt.* **31**, 5666 (1992)
3. J.J. Amodei, D.L. Staebler: *Appl. Phys. Lett.* **18**, 540 (1971)
4. H. Vormann, G. Weber, S. Kapphan, E. Krätzig: *Solid State Commun.* **40**, 543 (1981)
5. A. Méndez, L. Arizmendi: *Opt. Mater.* **10**, 55 (1998)
6. R. Müller, M.T. Santos, L. Arizmendi, J.M. Cabrera: *J. Phys. D: Appl. Phys.* **27**, 241 (1994)
7. R. Müller, J.V. Alvarez-Bravo, L. Arizmendi, J.M. Cabrera: *J. Phys. D: Appl. Phys.* **27**, 1628 (1994)
8. L. Arizmendi, E.M. de Miguel-Sanz, M. Carrascosa: *Opt. Lett.* **23**, 960 (1998)
9. A. Van der Lugt: *IEEE Trans. Inf. Theory* **IT-10**, 139 (1964)
10. M.C. Lasprilla, S. Granieri, N. Bolognini: *Optik* **105**, 61 (1997)
11. F.T.S. Yu, S. Yin: *Opt. Eng.* **34**, 2224 (1995)
12. H. Kogelnik: *Bell Syst. Tech. J.* **48**, 2909 (1969)
13. H. Kurz, E. Krätzig, W. Keune, H. Engelman, U. Gonser, B. Dischler, A. Räuber: *Appl. Phys.* **12**, 355 (1977)
14. R. Müller, L. Arizmendi, M. Carrascosa, J.M. Cabrera: *Appl. Phys. Lett.* **60**, 3212 (1992)